Acta Cryst. (1996). D**52**, 722–729

Molecular Rigid-Body Displacements in a Tetragonal Lysozyme Crystal Confirmed by X-ray Diffuse Scattering

JAVIER PÉREZ, PHILIPPE FAURE AND JEAN-PIERRE BENOIT

LURE, Laboratoire CNRS-CEA-MENESR, Bâtiment 209D, Université Paris-Sud, F-91405 Orsay, France. E-mail: perez@lure.u-psud.fr

(*Received 1 December 1995; accepted 21 February 1996*)

Abstract

X-ray diffuse scattering from protein crystals is, at the moment, the only available experimental process to be directly sensitive to long-range correlations between protein-atom displacements. It is shown here that calculations based on independent rigid-body displacements of individual molecules yield a description in good agreement with the experimental diffuse-scattering pattern displayed by tetragonal crystals of hen egg-white lysozyme (HEWL) In particular, it appears that molecular rigid-body translations and rigid-body rotations appear roughly in the same proportion as the average atomic mean-square positional fluctuations. The crystallographic temperature-factor analysis by TLS (translation/libration/screw) refinement, performed by Sternberg, Grace & Phillips [Sternberg, Grace, & Phillips (1979). *J. Mol. Biol.* **130**, 231–253], is then confirmed and completed by a quantitative estimation of the molecular rigid-body translation contributions. The major contribution of molecular rigid-body displacements to the average atomic mean-square positional fluctuations, contradicts a previous analysis of the tetragonal HEWL diffuse-scattering data by Clarage, Clarage, Phillips, Sweet & Caspar [Clarage, Clarage, Phillips, Sweet & Caspar (1992). *Proteins Struct. Funct. Genet.* **12**, 145–157] which concluded that short-range correlations dominate. The origin of these opposite conclusions mostly lies in the different hypotheses made to model diffuse scattering, underlying the limits of the 'homogeneous disorder' model.

1. Introduction

X-ray crystallography has proved to be a very efficient tool in the determination of three-dimensional protein structures. For some structures, this extends to atomic resolution, where anisotropic atomic mean-square fluctuations can be revealed, through anisotropically refined temperature factors (*B* factors) (Yamano & Teeter, 1994; Teeter, Roe & Heo, 1993). Knowing the importance of dynamics in protein biological mechanisms (Janin & Wodak, 1983), it is a matter of interest to see to what extent an X-ray scattering experiment may also contribute to the analysis of the spatial correlations between the atomic displacements. Strictly speaking, temperature factors do not give information about correlations between the atomic displacements, but for those residues where the anisotropy of the atomic fluctuations is clearly defined, it is possible to infer the global character of the residue displacement. However, the analysis of the anisotropic *B* factors provides little information about the correlations between the displacements of different residues, so that the range of correlations which can be investigated in this way is strongly limited. Moreover, for most protein structures, only isotropically averaged values of the *B* factors are available.

The TL model (translation/libration) developed for molecular crystals in the 1950's (Cruickshank, 1956*a*,*b*) extended to the full TLS model (translation/libration/screw) by Schomaker & Trueblood (1968), was later generalized to protein crystals as a first attempt to carry out an interpretation of the thermal factors in terms of correlated displacements (Artymiuk *et al.*, 1979; Howlin, Moss & Harris, 1989; Kuriyan & Weis, 1991; Harris, Pickersgill, Howlin & Moss, 1992). More sophisticated molecular-dynamics computer calculations were used later with this objective (for a critical approach, see Hünenberger, Mark & van Gunsteren, 1995). Yet, interesting as these models may be, they can only remain a likely hypothesis, as long as direct measurements of the displacement correlations are not made.

Contrasting with Bragg crystallography, X-ray diffuse scattering is directly sensitive to these correlations (Amorós & Amorós, 1968). Experimental difficulties because of its weak intensity seriously hampered the development of this technique, but the availability of modern detectors, such as imaging plates, coupled with the high flux from a synchrotron source, has made measurements of diffuse scattering intensities in protein crystals feasible. Two review papers on X-ray diffuse scattering from proteins crystals have been recently published (Benoit & Doucet, 1995; Moss & Harris, 1995). Three different X-ray diffuse-scattering features may be distinguished, thermal diffuse scattering (TDS), diffuse streaks, and cloudy diffuse scattering (Glover, Harris, Helliwell & Moss, 1991). TDS is essentially situated around Bragg peaks, and arises from correlations over many cells in the crystal. TDS can always be detected in a protein diffraction pattern, and the precise analysis

ISSN 0907-4449

of its profile may provide information on the degree of harmonicity of phonons propagating within the crystal (Amorós & Amorós, 1968). Diffuse streaks, located along reciprocal lattice planes, derive from correlations expanding over particular rows of molecules, involving a small group of cells (Doucet & Benoit, 1987). Finally, cloudy diffuse scattering is not linked to any reciprocal lattice symmetry, and arises from correlations which do not exceed the size of a unit cell.

In recent years, several papers have been devoted to the interpretation of cloudy diffuse scattering in terms of correlated motion (Caspar, Clarage, Salunke & Clarage, 1988; Chacko & Phillips, 1992; Clarage, Clarage, Phillips, Sweet & Caspar, 1992; Mizuguchi, Kidera & Go, 1994; Kolatkar, 1994; Faure *et al.*, 1994). In the present work, we focus on the analysis of cloudy diffuse scattering arising from a tetragonal hen egg-white lysozyme (HEWL) crystal. We show that it is well accounted for, by considering a model of rigid-body molecular displacements. Furthermore, this model has also been succesfully used to fit the major part of *B*-factor main-chain fluctuations (Artymiuk *et al.*, 1979, Sternberg, Grace & Phillips, 1979). The comparison between the atomic mean-square fluctuations deduced from diffuse scattering and thermal factors corroborates the Artymiuk *et al.* interpretation of the crystallographic thermal factors and allows a quantization of the diffuse intensity.

2. Methods and results

Tetragonal crystals of HEWL show intense 'cloudy' diffuse scattering, mostly concentrated in a ring at about 3.7 Å resolution. Fig. 1 shows part of an experimental pattern, where diffuse scattering is particularly structurated???. The intensity of diffuse scattering is of the same order of magnitude as the scattering resulting from the capillary and the solvent surrounding the crystal. These 'parasitic' contributions were subtracted from the untreated pattern, after measuring them separately in the same geometrical conditions as for the crystal.

To fit the experimental diffuse-scattering pattern, we propose here a simple model of molecular rigid-body isotropic translations and rotations (iso-TL). In the present model, the molecules within the crystal are considered to move as rigid bodies, independently from each other. This means that, as a first approximation, we do not take into account possible intramolecular deformations, nor the coupling between adjacent molecules in the crystal. The hypothesis of isotropy was also taken as a first estimation, as we are less interested for the moment in precise anisotropic refinement than in the relevance of the TL model.

According to the formalism originally proposed by Guinier (1963), and further developed by Doucet & Benoit (1987) for protein crystals, diffuse scattering can be derived from explicit models of displacements. The most compact and general way to write the fundamental equation of diffuse scattering is,

$$I_D(\mathbf{S}) = \sum_{p=1}^{M} (\langle |F_p|^2 \rangle - |\langle F_p \rangle|^2), \qquad (1)$$

where $I_D(\mathbf{S})$ gives the diffuse intensity at the end of the scattering vector $\mathbf{S}$, and the summation is over the M groups of atoms, D_p, which are considered to bear correlated displacements. F_p represents the structure factor of one of the possible configurations of the group of atoms, D_p, and the average is made over all these possible configurations. Further details are given now on the iso-TL simulations.

2.1. *Isotropic translations*

In the case of rigid translations, (1) simplifies to,

$$I_D(\mathbf{S}) = \sum_p |F_p(\mathbf{S})|^2 \{1 - \exp[-4\pi^2 \langle (\mathbf{S}.\mathbf{u}_p)^2 \rangle]\} \qquad (2)$$

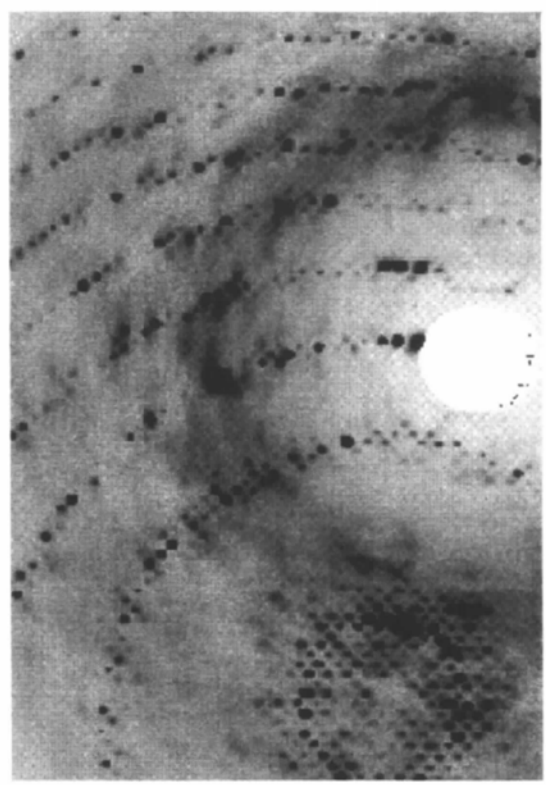

Fig. 1. Part of an experimental diffraction pattern from a tetragonal hen egg-white lysozyme crystal ($P4_32_12$, a = 79.02, c = 38.05 Å), numerically corrected from the parasitic scattering of capillary and solvent. The orientation of the crystal was chosen to show a high amount of cloudy diffuse scattering. The Bragg spots are saturated on purpose. Data were collected at station DW32 of the wiggler beamline at the LURE-DCI synchrotron (Orsay, France), with monochromated X-rays, λ = 0.9 Å. A MAR Research imaging-plate was used as detector.

To simulate diffuse scattering from isotropic translations, (2) was used, replacing $\langle(\mathbf{S}.\mathbf{u}_p)^2\rangle$ by $(S^2.u_0^2)/3$ for each of the eight molecules of the unit cell. The root-mean-square displacement u_0 was taken to equal 0.5 Å, but as its value hardly influences the pattern structuring, the choice made here is only a likely order of magnitude. The resulting pattern is shown in Fig. 2(*a*). Bragg peaks are represented as white spots.

2.2. *Isotropic rotations*

Isotropy has been approximated for small rotations by three independent rotations around three mutually perpendicular axes, crossing at the centre of mass (we used the crystallographic axes). The calculation of $I_D(\mathbf{S})$ from an axial rotation model was made in two steps. Starting from the crystallographic coordinates of each molecule, we set two rotated configurations of the atoms, symmetrical about the crystallographic configuration. Then, according to (1), we computed numerically the averages over the structure factors corresponding to these 'displaced' structures. We have verified that introducing more intermediate configurations does not modify substantially the simulated pattern.

For each of the three axes, diffuse scattering was calculated, according to the two-step process just described, with a constant angle of 1.5°. After summation of these partial terms, the purchased simulation was obtained, and is shown in Fig. 2(*b*).

2.3. *Superposition of translations and rotations*

In Figs. 2(*a*) and 2(*b*), the 64 grey levels were scaled independently so no comparison concerning the relative intensities between these two figures should be made. These patterns have to be compared separately with the experimental one in Fig. 1. At first sight, it appears that, in both cases (Figs. 2*a* and 2*b*), the patches of high diffuse intensity are situated at places where experimental diffuse scattering is indeed observed. Moreover, by combining them, complementarity between the respective features results in a better

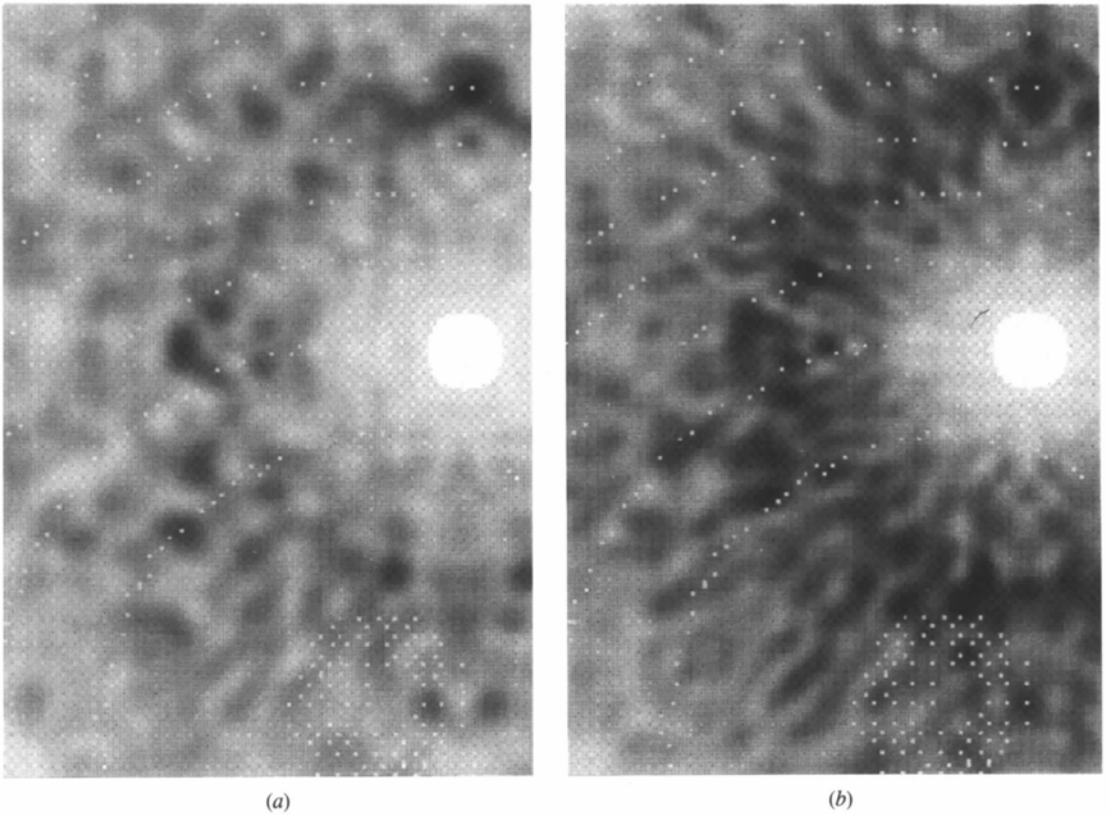

(*a*) (*b*)

Fig. 2. Simulated diffuse-scattering patterns, corresponding to the same orientation as in Fig. 1. Two different kinds of displacements are used: (*a*) independent rigid-body isotropic translations of each of the eight proteins of the unit cell, with an arbitrary mean-square displacement of 0.25 Å^2; (*b*) independent rigid-body isotropic rotations of each of the eight proteins of the unit cell, about their respective mass center, with an arbitrary mean-square displacement of 0.25 Å^2. The grey levels are scaled, for each of the simulations, to the respective maximum intensities. Thus, although the chosen mean-square displacements are the same (*i.e.*, the average intensities are equal), the two figures cannot directly be compared in a quantitative way.

fitting of the experimental pattern. The best proportion derived from a visual examination corresponds roughly (±25%) to the same average intensities of each simulation. The resulting pattern is shown in Fig. 3. Here, not only the general aspect of the experimental frame is retained, but very peculiar features of it are quite nicely reproduced, like the very intense meridional and equatorial patches. More strikingly the combination of the two simulations leads to the formation of the diagonally elongated strip, situated in the north-west direction. This good correspondence between simulation and experience then strongly suggests the relevance of the simple model of molecular TL displacements.

2.4. *Comparison with thermal factors*

Since the average diffuse intensity is roughly proportional to the mean-square displacement amplitude, the combination used for Fig. 3 simply corresponds to equal (±25%) mean-square amplitudes for rotations and for translations, both types of displacements being independent. However, no absolute value of the mean-square displacement can be derived from the diffuse-scattering analysis. Therefore, both to check the coherence between our model and the crystallographic refinement, and to get quantitative values of the displacements involved, we compared the atomic mean-square fluctuations given by the *B* factors and the fluctuations derived from the iso-TL model.

Fig. 4 shows the crystallographic main-chain positional fluctuations deduced from the refined isotropic *B* values by the relation $B_i = 8\pi^2\langle u_i^2\rangle$. The data are taken from a refinement performed at 295 K by Kurinov & Harrison (1995), at a resolution of 1.7 Å. In this work, the authors compared the refined structures of tetragonal lysozyme at six different temperatures in the range 95–295 K. It was shown that, in spite of a significant volume change of the unit cell, the variation of the structure of the protein involves only small relative displacements of structure elements. The authors showed that, resulting from an increase of lattice disorder at low temperatures, the overall thermal factor does not significantly depend on temperature, with a total mean-square displacement of 0.27 Å^2 at 295 K. It is interesting to note that, in an earlier study, a refinement made at a resolution of 2.0 Å, resulted in the same variations of the positional fluctuations against residue number, although the average *B* factor, with a total mean-square displacement of 0.17 Å^2, was much lower (Young, Dewan, Nave & Tilton, 1993). This discrepancy in the average *B* factor is not necessarily surprising, since this value is very dependent on the data-collection quality. More comforting is the fact that the variations of the *B* factors along the chain do not depend on the refinement used.

As expected from the TLS refinement performed by Artymiuk *et al.* (1979), the rigid-body model is in

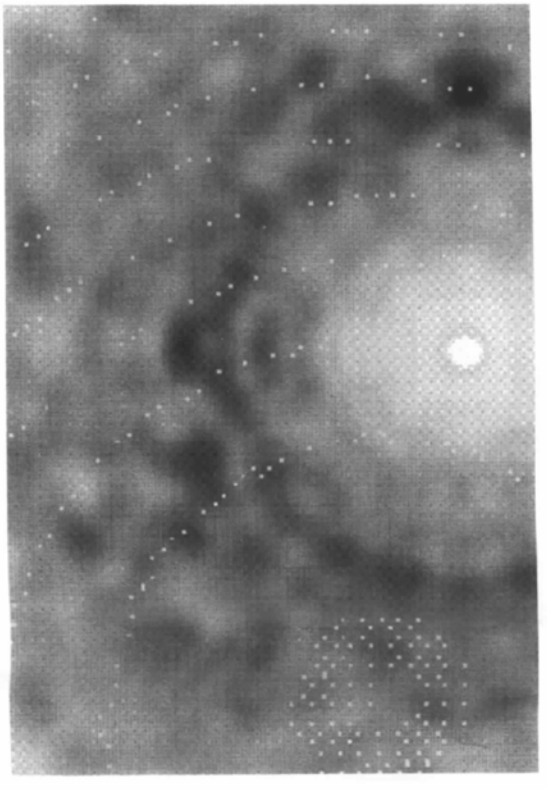

Fig. 3. Simulated diffuse-scattering pattern, taking account of both rigid-body translations and rigid-body rotations of each protein in the unit cell, independently of its neighbours. An arbitrary total mean-square displacement of 0.5 Å^2 was taken to produce this pattern, and the grey levels are scaled to the maximum intensity. The average mean-square displacement is the same for each of the two kinds of displacements. This proportion gives the best visual agreement with the experimental pattern (Fig. 1). In particular, the diagonally elongated strip, situated in the north-west direction of the figure (see text), is clearly visible.

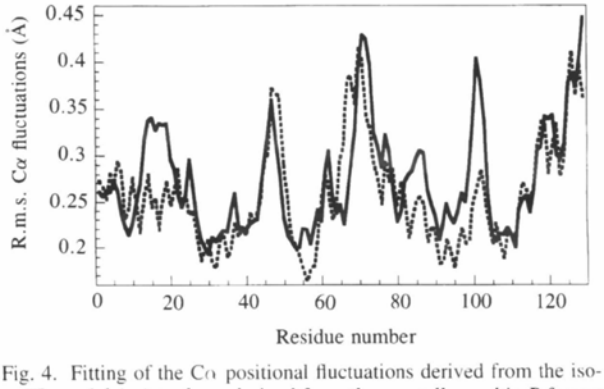

Fig. 4. Fitting of the Cα positional fluctuations derived from the iso-TL model (- -) to those derived from the crystallographic *B* factors (—). The displacement amplitudes used for the iso-TL model are, a 0.1 Å^2 mean-square displacement for the rigid-body rotations, and a translation-like mean-square displacement of 0.16 Å^2. From the diffuse-scattering analysis, it is deduced that 0.1 Å^2 of these 0.16 Å^2 result from rigid-body molecular translations.

good agreement with an important part of the *B*-factor fluctuations. As rigid-body translations result in the same displacement for all atoms, rigid-body rotations can be used alone and separately to fit the *B*-factor variations. Hence, by changing the rotation mean-square displacement $\langle u^2_{\text{rot}} \rangle$, it is possible to modulate the proportions between the atomic fluctuations. The value of the mean-square displacement which allows us to fit best the crystallographic *B*-factor fluctuations is equal to 0.1 Å^2, corresponding to a mean-square angle of axial rotation of 0.8°[2]. The superposition of the *B*-factor fluctuations from both the crystallographic refinement and the TL model are shown on Fig. 4. A global shift of 0.16 Å^2 was applied to the rigid rotation fluctuations to bring both curves in correct superposition. Part of this shift corresponds to molecular rigid translations. According to the value found for $\langle u^2_{\text{rot}} \rangle$, and from the diffuse-scattering analysis, the amount of rigid translations can be deduced *a posteriori* to near 0.1 Å^2. Finally, about 0.07 Å^2 mean-square fluctuation has not been taken into account by our model.

3. Discussion

In their best fitting of the plot of the main-chain temperature factor *versus* residue number by a refined TLS model (anisotropic translation/libration/screw), Sternberg *et al.* (1979) did not manage to account fully for the observed fluctuations. Actually, this is not surprising, at least since the internal deformations of the protein have been omitted. The fact remains that the TLS model appears to fit an important part of the atomic fluctuations extremely well. Then, the simplicity of the model and the fact that it is physically acceptable, make it very attractive. However, it is impossible to really prove the relevance of any displacement model by a simple *B*-factor analysis, since *B* factors are not sensitive to the atomic displacement correlations. This is why the present diffuse-scattering analysis may be useful to prove the effective existence of molecular rigid-body displacements in HEWL tetragonal crystals.

The present diffuse-scattering results show that rigid-body molecular translations and rotations contribute in the same proportion to a significant portion of the average atomic displacements. It is worth noting that no hypothesis concerning the existence of molecular translational displacements could be made from the *B*-factor variations, since such displacements lead to the same atomic thermal factor for all atoms. Only diffuse scattering allowed us to state that rigid translations are indeed present in HEWL tetragonal crystals. Conversely, the existence of molecular rotations could be supposed *a priori* from the analysis of the *B*-factor fluctuations. But again, the direct confirmation given by diffuse scattering of the existence of such movements is essential, in particular because it allows differentiation between models giving the same *B*-factor fluctuations. For example, the simulation of a pattern derived from a superposition of rigid translations and of a breathing motion of the proteins, the alternative model proposed by Sternberg *et al.*, results in a much poorer agreement with diffuse-scattering experimental data (Fig. 5).

Yet, the quantitative values for the rigid-body displacement amplitudes, derived here from the comparison with the *B* factors, should be considered with care. These values were deduced from the best possible fitting of a great part of the *B*-factor fluctuations by the iso-TL model. But our quantitative analysis is correct only if that part of the *B*-factors which is well fitted by the TL model is indeed entirely due to rigid-body displacements. In particular, we cannot eliminate completely the possible existence of another type of displacement, which in some proportion would contribute to the *B*-factor fluctuations in the same way as the TL model. Only a precise analysis of both Bragg and diffuse-scattering intensities could lead to an absolute quantization of the TL displacement amplitudes.

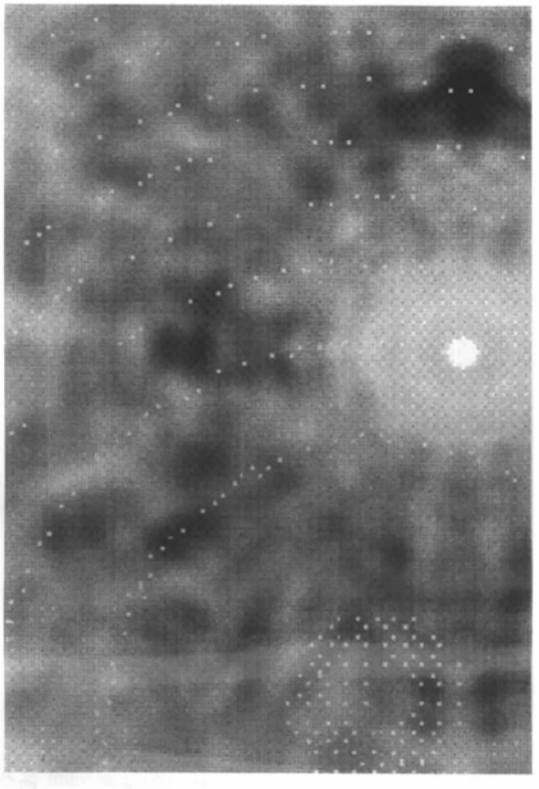

Fig. 5. Simulated diffuse-scattering pattern, taking account of both isotropic rigid-body translations and breathing mode of each protein in the unit cell, independently of its neighbours. An arbitrary total mean-square displacement of 0.5 Å^2 was taken to produce this pattern, and the grey levels are scaled to the maximum intensity. As in Fig. 3, the average mean-square displacement is the same for each of the two kinds of displacements. The breathing mode brings no visible improvement in the agreement with the experimental pattern, compared with isotropic rigid-body translations alone (Fig. 2*a*).

3.1. *Can intramolecular displacements be revealed?*

From HEWL orthorhombic crystals, diffuse streaks, as well as cloudy diffuse scattering are observed. Diffuse streaks arise from translations of rows of molecules (Doucet & Benoit, 1987), correlated over many cells, while the very diffuse scattering, in particular observed between these planes, is mostly due to intramolecular correlations, and can be analysed using normal mode calculations (Faure *et al.*, 1994). On the other hand, there are no diffuse streaks in the diffuse-scattering pattern of tetragonal crystals. Here, the displacements of the whole molecules are not correlated from cell to cell, and contribute to the cloudy diffuse scattering, not to restrained diffuse streaks. Therefore, the intramolecular displacements, which in any case result in cloudy diffuse scattering, produce here a contribution which is masked, in great part, by the more intense cloudy TL contribution. For this reason, it is difficult to collect information about the intramolecular displacement correlations in tetragonal crystals of HEWL. Moreover, because of the high number of protein molecules per unit cell (eight), the diffuse scattering arising from intramolecular displacements is considerably smoothed (normal-mode simulations, not shown). It would then be quite difficult to correctly fit their contribution to the experimental data. A possible way to access to the intramolecular correlations, would be to take several neighbouring molecules into account in a normal mode analysis. In this way, the relationship between molecular and intramolecular displacements could be calculated.

3.2. *Comparison with previous results on tetragonal HEWL*

At odds with our results, Clarage *et al.* (1992) underline the predominance of short-range correlated homogeneous disorder in tetragonal HEWL crystals (correlation length of about 6 Å). Their conclusions were also derived from X-ray diffuse-scattering experiments, and the closeness between their patterns and ours immediately dismisses possible experimental differences. To see how interpretations of the same diffuse-scattering data may lead to so different diagnostics, a short review is necessary about the method used by Clarage *et al.* to analyse the experimental data, method based on a 'homogeneous correlation' model.

Within the harmonic approximation, the diffuse intensity is given by the following formula,

$$I_D(\mathbf{S}) = \sum_{n,n'}\sum_{a,a'} f_a(S)\exp[-W_a(\mathbf{S})]f_{a'}(\mathbf{S})\exp[-W_{a'}(\mathbf{S})] \times \exp[i2\pi\mathbf{S}.(\mathbf{t}_n - \mathbf{t}_{n'})]\exp[i2\pi\mathbf{S}.(\mathbf{r}_a - \mathbf{r}_{a'})] \times \{\exp[4\pi^2\langle(\mathbf{S}.\mathbf{u}_{a,n})(\mathbf{S}.\mathbf{u}_{a',n'})\rangle] - 1\}, \quad (3)$$

where $\exp(-W_a)$ is the atomic Debye–Waller factor and $W_a = 2\pi^2\langle(\mathbf{S}.\mathbf{u}_{a,n})^2\rangle$. As was clearly pointed out by Mizuguchi *et al.* (1994) the information concerning the correlations between the atomic displacements is concentrated in the terms $\langle(\mathbf{S}.\mathbf{u}_{a,n})(\mathbf{S}.\mathbf{u}_{a',n'})\rangle$, which are directly related to the (3×3) covariance matrices $\langle\mathbf{u}_{a,n}\mathbf{u}_{a',n'}^T\rangle$ by $\langle(\mathbf{S}.\mathbf{u}_{a,n})(\mathbf{S}.\mathbf{u}_{a',n'})\rangle = \mathbf{S}^T\langle\mathbf{u}_{a,n}\mathbf{u}_{a',n'}^T\rangle\mathbf{S}$.

In the 'homogeneous correlation' model, $\langle\mathbf{u}_{a,n}\mathbf{u}_{a',n'}^T\rangle$ is a *priori* reduced to,

$$\langle u^2\rangle\Gamma(||\mathbf{r}_a - \mathbf{r}_{a'}||) \times \begin{pmatrix} 1 & 0 & 0 \\ 0 & 1 & 0 \\ 0 & 0 & 1 \end{pmatrix},$$

where $\Gamma(r) = \exp(-r/\gamma)$, and γ is the relaxation distance of the correlation function. In other words, whereas, in our structural approach, the simulated diffuse scattering is derived from peculiar models of concerted displacements, Clarage *et al.* in a kind of statistical approach, make use of an *a priori* positive correlation function, $\Gamma(r)$, decreasing with the interatomic distance and with few parameters to be refined (essentially the 'correlation length', γ). Two fundamental consequences derive from this approach. First, as the off-diagonal terms of the cross-correlated matrices are virtually zeroed, non-colinear correlated displacements (occuring in rotations, for example, or in any normal mode of vibration) are *a priori* excluded. Secondly, since the $\Gamma(r)$ function is taken positive, it is supposed that shearing-type correlations, with two atoms moving in the same direction but in opposite ways, are not considered either. For these two reasons, the patterns simulated from the Γ-function approach always reproduce smeared versions of the rigid translation pattern (where all displacements are colinear and of the same amplitude), the degree of smearing depending on how stiff $\Gamma(r)$ decreases with r. Precisely, the lower the relaxation length, γ, the more the pattern is smeared (Mizuguchi *et al.*, 1994).

To analyse the cloudy diffuse scattering from HEWL tetragonal crystals, Clarage *et al.* propose a model based solely on the Γ-function formalism. The simulated pattern is smeared to the extent required so as to roughly account for the various experimental diffuse patches by decreasing the value of γ. In the absence of relevant agreement factors, it is difficult here to discuss to which degree the simulated pattern reproduces correctly the experimental data, and in particular, to compare it to our simulation. Indeed, as can be seen from our simulations, the superposition of diffuse features arising from diverse types of displacements also leads to a decrease of the pattern level of structuring, *i.e.* giving also the impression of a smooth diffuse scattering. However, in our opinion, trying to account for diffuse-scattering features solely by smearing the pattern derived from rigid translation correlations can lead to an arbitrary interpretation of the experimental data. Actually, there is no reason why non-colinear correlations should be here neglected with regards to translational correlations. The simulated pattern might, therefore, be smeared too far and artificially include the diffuse patches due to the other kinds of

correlations (rotations, . . .). In consequence, the cloudy diffuse scattering may be wrongly interpretated in terms of correlations, because it is forced, with no further justification (as, for example, involving a comparison with the *B*-factor fluctuations), to include translation-type correlations only.

In any case, the treatment of the cloudy diffuse-scattering data should require the least biased models of correlated displacements. When possible, other external considerations, such as the physical relevance of the model or possible comparisons with the *B*-factor fluctuations should be included. This is what we have tried to do in this work, we have considered simple but still physically acceptable kinds of displacements, namely rigid-body displacements, and reinforced our choice by the results of the analysis of the crystallographic *B*-factor fluctuation, (*i.e.* as previously performed by Sternberg *et al.*, 1979).

4. Conclusions

We have shown here that, for the tetragonal crystal form of lysozyme, simulations using rigid-body molecular displacements provide a good interpretation of the experimental diffuse-scattering data. We were able to quantify the proportion of the total mean-square displacement which can be attributed to rigid displacements of independent molecules by comparing the main-chain positional atomic fluctuations obtained by the crystallographic refinement to those deduced from rigid-body molecular rotations and translations.

The high proportion of rigid-body displacements which is deduced, about 70% in mean-square amplitude of the average atomic fluctuations (global *B* factor), strongly contradicts previous interpretations of tetragonal lysozyme diffuse-scattering data in terms of homogeneous disorder (Clarage *et al.*, 1992). To our understanding, this discrepancy mostly lies in the fact that the type of correlation accounted for by homogeneous disorder models is intrinsically limited, which thus may lead to an erroneous interpretation of the experimental diffuse scattering. This limitation vanishes when diffuse scattering is directly simulated from models of atomic displacements. Among such models, rigid-body displacements offer a simple, but still physically meaningful, approximation of more complicated correlations.

An important question which cannot be answered by a single diffuse-scattering analysis concerns the dynamic character of the molecular displacements. Of particular interest would be to observe the effect of the harmonic/anharmonic transition at *ca* 200 K, which has been shown to occur, by experimental methods sensitive to dynamics in crystals of myoglobin (Doster, Cusack & Petry, 1989) and in tetragonal lysozyme (Kurinov, Krupianskii, Suzdalev & Goldanskii, 1987). This transition should imply a sudden decrease in the slope of the dynamic part of the overall thermal factors *versus* temperature, when the temperature is decreased through 200 K. This phenomenon has indeed been observed for the complete (dynamic + static) overall thermal factor in ribonuclease A crystals (Tilton, Dewan & Petsko, 1992). However, a recent examination of the behaviour of tetragonal lysozyme crystals by Kurinov & Harrison (1995) shows a quite small modification of the total overall *B* factor with temperature. This has been interpreted as the appearence and the increase of a static disorder with decreasing temperature. The evolution of diffuse-scattering features arising from static disorder should be striking enough to yield new information. For this purpose, it would then be worth investigating the temperature behaviour of the diffuse-scattering pattern from a HEWL tetragonal crystal.

References

Amorós, J. L. & Amorós, M. (1968). *Molecular Crystals: Their Transforms and Diffuse Scattering*. New York: John Wiley.

Artymiuk, P. J., Blake, C. C. F., Grace, D. E. P., Oatley, S. J., Phillips, D. C. & Sternberg, M. J. E. (1979). *Nature (London)*, **280**, 563–568.

Benoit, J. P. & Doucet, J. (1995). *Q. Rev. Biophys.* **28**(2), 131–169.

Caspar, D. L. D., Clarage, J. B., Salunke, D. M. & Clarage, M. S (1988). *Nature (London)*, **332**, 659–662.

Chacko, S. & Phillips, G. N. (1992). *Biophys. J.* **61**, 1256–1266.

Clarage, J. B., Clarage, M. S., Phillips, W. C., Sweet, R. M. & Caspar, D. L. D. (1992). *Proteins Struct. Funct. Genet.* **12**, 145–157.

Cruickshank, D. W. J. (1956*a*). *Acta Cryst.* **9**, 747–753.

Cruickshank, D. W. J. (1956*b*). *Acta Cryst.* **9**, 754–756.

Doster, W., Cusack, S. & Petry, W. (1989). *Nature (London)*, **337**, 754–756.

Doucet, J. & Benoit, J. P. (1987). *Nature (London)*, **325**, 643–646.

Faure, Ph., Micu, A., Perahia, D., Doucet, J., Smith, J. C & Benoit, J. P. (1994). *Nature Struct. Biol.* **1**, 124–128.

Glover, I. D., Harris, G. W., Helliwell, J. R. & Moss, D. S. (1991). *Acta. Cryst.* B**47**, 960–968.

Guinier, A. (1963). *X-ray Diffraction*. San Francisco: Freeman.

Harris, G. W., Pickersgill, R. W., Howlin, B. & Moss, D. S. (1992). *Acta Cryst.* B**48**, 67–75.

Howlin, B., Moss, D. S. & Harris, G. W. (1989). *Acta Cryst.* A**45**, 851–861.

Hünenberger, P. H., Mark, A. E. & van Gunsteren, W. F. (1995). *J. Mol. Biol.* **252**, 492–503.

Janin, J. & Wodak, S. J. (1983). *Prog. Biophys. Mol. Biol.* **42**, 21–78.

Kurinov, I. V., Krupianskii, Yu, F., Suzdalev, I. P. & Goldanskii, V. I. (1987). *Hyperfine Interact.* **33**, 223–232.

Kurinov, I. V. & Harrison, R. W. (1995). *Acta Cryst.* D**51**, 98–109.

Kuriyan, J. & Weis, W. I. (1991). *Proc. Natl Acad. Sci. USA*, **88**, 2773–2777.

Mizuguchi K., Kidera A. & Go, N. (1994). *Proteins Struct. Funct. Genet.* **18**, 34–48.

Moss, D. S. & Harris, G. W. (1995). *Radiat. Phys. Chem.* **45**, 523–535.

Schomaker, V. & Trueblood, K. N. (1968). *Acta Cryst.* B**24**, 63–76.
Sternberg, M. J. E., Grace, D. E. P. & Phillips, D. C. (1979). *J. Mol. Biol.* **130**, 231–253.
Teeter, M. M., Roe, S. M., & Heo, N. H. (1993). *J. Mol. Biol.* **230**, 292–311.
Tilton, R. F., Dewan, J. C. & Petsko, G. A. (1992). *Biochemistry*, **31**, 2469–2481.
Yamano, A. & Teeter, M. M. (1994). *J. Biol. Chem.* **269**, 13956–13965.
Young, A. C. M., Dewan, J. C., Nave, C. & Tilton, R. F. (1993). *J. Appl. Cryst.* **26**, 309–319.